Journal of Alloys and Compounds 534 (2012) 25–31

Contents lists available at SciVerse ScienceDirect

Journal of Alloys and Compounds

journal homepage: www.elsevier.com/locate/jalcom

Determination of the transition to the high entropy regime for alloys of refractory elements

Mariela F. del Grosso [a,b,c], Guillermo Bozzolo [d,*], Hugo O. Mosca [a,c]

[a] Gerencia de Investigación y Aplicaciones, Comisión Nacional de Energía Atómica, Av. Gral. Paz 1499 (B1650KNA), San Martín, Argentina
[b] CONICET, Buenos Aires, Argentina
[c] Grupo de Caracterización y Modelización de Materiales, UTN, FRGP, H. Yrigoyen 288, (B1617FRG) Gral. Pacheco, Argentina
[d] Loyola University Maryland, 4501 N. Charles St., Baltimore, MD 21210, USA

ARTICLE INFO

Article history:
Received 8 December 2011
Received in revised form 14 March 2012
Accepted 17 April 2012
Available online 26 April 2012

Keywords:
High entropy alloys
Atomic scale structure
Computer simulations

ABSTRACT

The development of high entropy alloys is currently limited to experimental work aimed at the determination of specific compositions that exhibit particular properties. The main feature of these alloys is their particular phase structure, which tends to be a continuous solid solution in spite of the large number of constituents which would otherwise form a large number of intermetallic phases. While it is known that equimolar concentrations and large number of elements are two necessary conditions for achieving high entropy behavior, not much is known regarding the transition to this regime in the presence of specific elements. Such knowledge would be useful when determining alloy compositions, as it would set boundaries for the necessary concentrations of each element in experimental situations. In this work, results of a computational modeling effort are presented, where a recently developed 5-element high entropy alloy of refractory elements is used as the foundation needed to examine such transition and determine the necessary lower bounds for the concentration of each element. Details of the phase structure of the quaternary combinations of W, Nb, Mo, Ta and V as they evolve upon the addition of a fifth element are discussed. The results are compared to the experimental case for the case of V added to W–Nb–Mo–Ta. Using these examples as a reference, the concept of critical concentrations for each element, signaling the transition to the high entropy regime, is developed, based on a simple analysis of only bulk properties of such alloys (lattice parameter, bulk modulus, and cohesive energy).

1. Introduction

The traditional approach for materials development focuses on a single base element or binary alloy with minority additions of several other elements in order to adjust its properties. Binary phase diagrams are very well known to great detail, so it is natural to start on the solid foundation provided by the ample experimental data available for these rather simple systems. In most alloy research programs using this starting point, materials end up being a combination of several elements, but the role of the minority additions can be, to a great extent, easily foreseen. While this approach can be carried on until the necessary properties are obtained, its reliance on one or two basic elements imposes a constraint that could eventually become an insurmountable obstacle, should the final result not meet the demands and expectations for that material. One alternative is to start from a different perspective, where several elements are simultaneously considered and further refinements are made from this starting point. However, unlike the traditional approach, this means dealing from the onset with systems for which the multicomponent phase diagrams are generally not known. Therefore, while this approach could result in new paths for the development of new materials, they bring an element of uncertainty that could be as limiting as the aforementioned problems can be in the usual approach.

Two recent developments might change this, as they are both directed towards eliminating such uncertainty when the system is based on a large number of basic elements, in nearly equal proportion. One is the fact that the high entropy of mixing of such multicomponent systems seems to favor the formation of extended solid solutions against the formation of intermetallic phases. Secondly, the increasing relevance of computational methods for multicomponent systems that allows for the inception, at very early stages of the alloy development, of necessary information about the basic system. This translates into more educated choices on the path to follow in the often long, tedious and costly process of adjusting the properties to the desired levels. In spite of these advantages, the research on so-called high entropy alloys (HEA) is still rather new and therefore relatively limited in scope and

* Corresponding author. Address: Physics Dept., Loyola University Maryland, 4501 N. Charles St., Baltimore, MD 21210, USA. Tel.: +1 410 995 4963.
E-mail address: guille_bozzolo@yahoo.com (G. Bozzolo).

0925-8388/$ - see front matter © 2012 Elsevier B.V. All rights reserved.
http://dx.doi.org/10.1016/j.jallcom.2012.04.053

options. It is, however, a field of rapid growth, given the typically unusual characteristics of these alloys, such as high strength and ductility, good wear, oxidation and corrosion resistance, making them appealing for a wide range of applications.

One key ingredient that is still missing in order to successfully and efficiently pursue this new line of research is the lack of tools to determine when a given multicomponent system assumes the characteristics typical of HEA, heretofore referred to as the transition to the high entropy regime. The natural starting point is, given a minimum number of elements (five or more), to choose equal concentrations for each constituent, thus maximizing the entropy of mixing. This is figuratively equivalent to start at the center of the multicomponent phase diagram where the high entropy regime is guaranteed. But from that point on, the experimental path gets exceedingly complicated when choices must be made in adjusting the concentration of each element in order to meet the desired goals in terms of properties. These adjustments must be made within the domain of high entropy behavior, but there are currently no tools to determine the allowed range of concentrations or, in other words, the phase field of the high entropy situation in the multicomponent phase diagram. Limitations such as cost, processing or desired properties could require establishing a wider field of options (i.e., minimum concentration of any given constituent) when determining the HEA composition. In this work, therefore, we apply an atomistic modeling approach to determine, from modeling data, the order parameters that govern these alloys and gain insight on the qualitative and quantitative features that lead to the characteristic high entropy effect. This effort is thus aimed at answering the question of what is the amount of each constituent needed to ensure HEA behavior, streamlining the trial and error approach characteristic of complex alloy development. The approach is based on the application of the Bozzolo–Ferrante–Smith (BFS) method for alloys [1,2] which is ideally suited for the atomistic study of multicomponent systems, as shown in previous applications to rather complex systems [3–7]. Therefore, based on experimental results and a straightforward modeling effort, it is the purpose of this work to introduce simple concepts that could allow for the determination of markers for such transition. To achieve this goal, we define an atomistic modeling framework centered on the study of a recently developed 5-element HEA with refractory elements and extract, from the modeling results, the relevant information to establish a procedure to describe the transition to the high entropy regime.

2. Background

Since the early work of Peker and Johnson [8] on the description of a 5-element Zr–Ti–Cu–Ni–Be alloy with exceptional glass forming ability, it has been recognized that alloys with five or more metallic elements in nearly equal proportions have promising properties. In the last decade, the number of systems studied experimentally has grown substantially [9,10]. Numerous compositions of n-element alloys ($n > 5$) have been studied experimentally [10–21], all showing that HEA tend to form simple crystal structures (bcc or fcc solid solutions or a combination of both). Experimental studies also include the role of constituents or alloying additions on properties [22–35]. However, relative to the extensive experimental work, theoretical work is somewhat lacking, limited to an analysis of the concepts and conditions underlying the field of HEA [36–38]. Yeh et al. [36] provided a novel way to classify alloys based on their number of constituents and the role played by the entropy of mixing. Zhang and Zhou [37] determined necessary conditions on entropy of mixing, atomic size, and enthalpy of mixing needed to be in the high-entropy regime. More recently, Wang et al. [38] studied the transformation from fcc to bcc based on atomic packing efficiency and lattice distortions and Zhang et al. suggested how to downselect potential alloying additions to 4- and 5-element fcc-based HEA (CoFeMnNi + X and CoFeMnNiSm + X) based on first-principles calculations and site occupancy schemes [39].

Due to the complexity of these systems, there is no current microscopic description of their structure and evolution and therefore, there is limited understanding on the transition to the high entropy regime upon changes in composition, number of elements, their concentrations, etc. In particular, nearly no theoretical or experimental work has been performed on HEA with refractory elements. To our knowledge, the only reported case is the recent work of Senkov et al. [40–42] motivated by the need of materials for aerospace applications with high melting temperatures. Their work on W–Nb–Mo–Ta and W–Nb–Mo–Ta–V HEA [40,41] revealed that a single phase bcc solid solution with exceptional microhardness and high melting temperature can be obtained. As a starting point towards the development of modeling tools for HEA, a theoretical analysis of this relatively simple HEA might yield light on the path to follow for the determination of new compositions for potential applications. With the exception of the Ta–V system, which forms a TaV_2 ordered phase at low temperatures, all the other binary combinations form continuous solid solutions, so it is not surprising that the 4- and 5-element alloys also stabilize in a rather featureless solid solution. Because of that, these W–Nb–Mo–Ta and W–Nb–Mo–Ta–V alloys might not be the best examples to demonstrate and quantify the high entropy effect but they certainly are, from a modeling standpoint, as they are simple enough (in terms of the number of constituents) to facilitate the investigation of those properties that ultimately lead to the typical HEA outcome.

3. Theory: the BFS method for alloys

The BFS method for alloys is a quantum approximate method based on the assumption that the energy of formation of a given atomic configuration is the sum of the individual atomic contributions, $\Delta H = \sum_i \varepsilon_i$. Each contribution ε_i consists of two terms: a strain energy, ε_i^s, which accounts for the change in geometry with respect to a single monatomic crystal of the reference atom i, and a chemical energy, ε_i^c, computed as if every neighbor of the atom i were in an equilibrium lattice site of a crystal of species i, but retaining its actual chemical identity. The computation of ε_i^s using Equivalent Crystal Theory (ECT) [43], involves three pure element properties for atoms of species i: cohesive energy (E_c), equilibrium lattice parameter (a) and bulk modulus (B_0). These three parameters for each of the constituent elements are needed in the general derivative structure of the final alloy (in this case, bcc). Additional ECT parameters, α and λ (see Ref. [43] for a detailed description of these parameters), can be easily derived from E_c, a, and B_0. The chemical energy, ε_i^c, accounts for the corresponding change in composition, considered as a defect in an otherwise pure crystal. The chemical 'defect' deals with pure and mixed bonds, therefore, two additional perturbative parameters, Δ_{AB} and Δ_{BA}, are needed to describe these interactions. A reference chemical energy, $\varepsilon_i^{c_0}$, is also included to insure a complete decoupling of structural and chemical features. Finally, the strain and chemical energies are linked with a coupling function, g_i, which ensures the correct volume dependence of the BFS chemical energy contribution. Therefore, the contribution of atom i to the energy of formation of the system is given by:

$$\varepsilon_i = \varepsilon_i^s + g_i(\varepsilon_i^c - \varepsilon_i^{c_0}). \quad (1)$$

First-principles calculations using the Linearized Augmented Plane Wave method [44] were used to determine the aforementioned single element parameters for W, Nb, Ta, Mo, and V, as well

as for the determination of the BFS perturbative parameters needed in the calculation of the chemical energy. These calculations involve the determination of the zero temperature equation of state of the pure solids (for the single element parameters) and the calculation of the energy of formation of the metastable B2 structures between the different binary combinations of all elements, from which the perturbative parameters, Δ_{AB} and Δ_{BA}, for every A–B pair can be obtained [5,6]. A preliminary modeling study of W–Nb–Mo–Ta and W–Nb–Mo–Ta–V alloys [45] reproduces the basic experimental findings in terms of phase structure and, consequently, validates the parameterization of the method as used in this work.

The evolution with temperature of the many systems studied in this work was performed via large scale Monte Carlo simulations using BFS for the energetics, dubbed BANN [3]. For brevity, we direct the reader to Refs. [1–3] for the necessary details of the method, the parameterization needed to perform the simulations, and operational equations as well as previous BFS applications to multicomponent systems [3–7]. The traditional Monte Carlo algorithm considers all possible swaps between atomic positions, accepted or rejected depending on a probabilistic factor $e^{-\frac{\Delta E}{kT}}$, where ΔE is the change in energy upon the atomic pair exchange. In the case of BANN, exchanges are restricted to only nearest-neighbor (NN) pairs, with their acceptance or rejection based on a probabilistic factor weighted by the available thermal energy, thus introducing information on the vibrational degrees of freedom.

It should be noted that all simulations are performed in rigid cells (i.e., uniform lattice parameter) although the lattice parameter is optimized at each temperature step. In addition, it should be pointed out that the term 'precipitate' used in the following description refers to regions of the cell where a unique and distinguishable atomic distribution is found, which may or may not translate into an actual precipitate that could be found in an experimental situation. It is, however, an indication that different atoms will search for specific distributions which, in certain experimental situations, could result in the precipitation of a second phase.

4. Results and discussion

4.1. Comparison of experiment and theory

Due to the fact that the WNbMoTa + V is the only case that was experimentally studied [40], this section deals with a detailed analysis of the transitional chain from $W_{27.3}Nb_{22.7}Mo_{25.6}Ta_{24.4}$ to $W_{19.9}Nb_{20.2}Mo_{21.0}Ta_{14.0}V_{25.0}$, with varying V concentration (x_V = 0, 2.5, 5.0,. . ., 25.0 at.%). This chain contains the experimental case, $W_{21.1}Nb_{20.6}Mo_{21.7}Ta_{15.6}V_{21.0}$. Simulation results reproduce and also predict a bcc solid solution for a wide temperature range, and yield bulk properties for the resulting bcc solid solution in good agreement with experimental measurements, as noted in Table 1, for the lattice parameter, density and melting temperature of the quaternary alloy and the five-element alloy with x_V = 21 at.%. Although the melting temperature was not determined experimentally, the work of Senkov et al. [40] provides computed values (T_m = 3177 K and 2946 K for the quaternary and the 5-element alloy, respectively) that are in good agreement with the BFS values, determined from the equation of state at zero temperature for either alloy as described in Ref. [6] (T_m = 3051 K and T_m = 2944 K, for the quaternary and the 5-element alloy with x_V = 21 at.%, respectively). Results for the melting temperature as a function of V concentration in W–Nb–Mo–Ta–V alloys (transitioning from the quaternary to 5-element alloys) are shown in Fig. 1. The agreement between experimental and theoretical values for these properties and the observed phase structure derived from the simulations suggest that the modeling framework and parameterization are appropriate to describe these systems.

Table 1
Experimental and theoretical values of the lattice parameter of the solid solution, density, and melting temperature for the quaternary and 5-element cases reported in Ref. [40].

	$W_{27.3}Nb_{22.7}Mo_{25.6}Ta_{24.4}$		$W_{21.1}Nb_{20.6}Mo_{21.7}Ta_{15.6}V_{21.0}$	
	Exp. (Ref. [40])	This work	Exp. (Ref. [40])	This work
Lattice parameter (Å)	3.2134	3.2289	3.1832	3.2000
Density (g/cm^3)	13.75 ± 0.03	13.79	12.36 ± 0.01	11.92
Melting temperature (K)	3177*	3051	2946*	2944

* Computed values.

Our preliminary analysis of these HEA [45] included modeling results for describing the evolution with temperature of the quaternary case and the experimentally studied case [40]. This description was made mostly in terms of the (short-range order) coordination matrices ρ_{AB} and μ_{AB}, which denote the probability that an atom A has an atom B as a nearest neighbor (NN), or as a next-nearest-neighbor (NNN), respectively. The results, displayed in Fig. 2, can be summarized by saying that there is a slow transition with descending temperature from a high temperature solid solution to a highly disordered pseudo-B2 structure, where each sublattice shows different population: one rich in Nb, and the other rich in Ta. The low impact of W and Mo in these results and, therefore, in the phase structure of this alloy, is a noticeable fact that shows that their presence is not as relevant as that of Ta, V, and Nb, in determining the transition to the high entropy regime. This transformation is apparent once Ta is 'activated' at intermediate temperatures (T < 1500 K), leading to the formation of Ta(W,Nb) precipitates. The temperature at which this process is in full force can be understood as a critical temperature, establishing a lower bound to the four-element solid solution. For much lower temperatures (T < 400 K), a second process takes place, when a Mo-rich precipitate forms. In all, it can be said that Ta dominates the behavior of the quaternary system and is solely responsible for the magnitude of the critical temperature and the resulting phase structure below that temperature.

The structure and temperature evolution of the 5-element alloy studied experimentally [33], $W_{21.1}Nb_{20.6}Mo_{21.7}Ta_{15.6}V_{21.0}$ (in at.%), was also described in terms of the coordination matrices [45]. As can be seen in Fig. 3, the probabilities are nearly equal to the concentration of each element in the mix, indicating that for T > 1000 K the system is in a completely disordered solid solution.

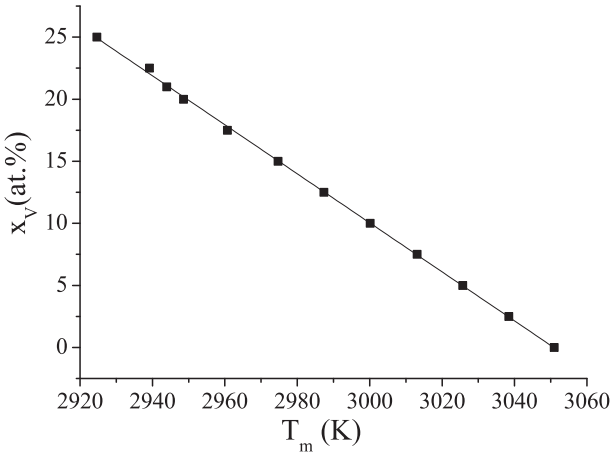

Fig. 1. Calculated values of the melting temperature T_m (in K) for W–Nb–Mo–Ta–V alloys as a function of V concentration.

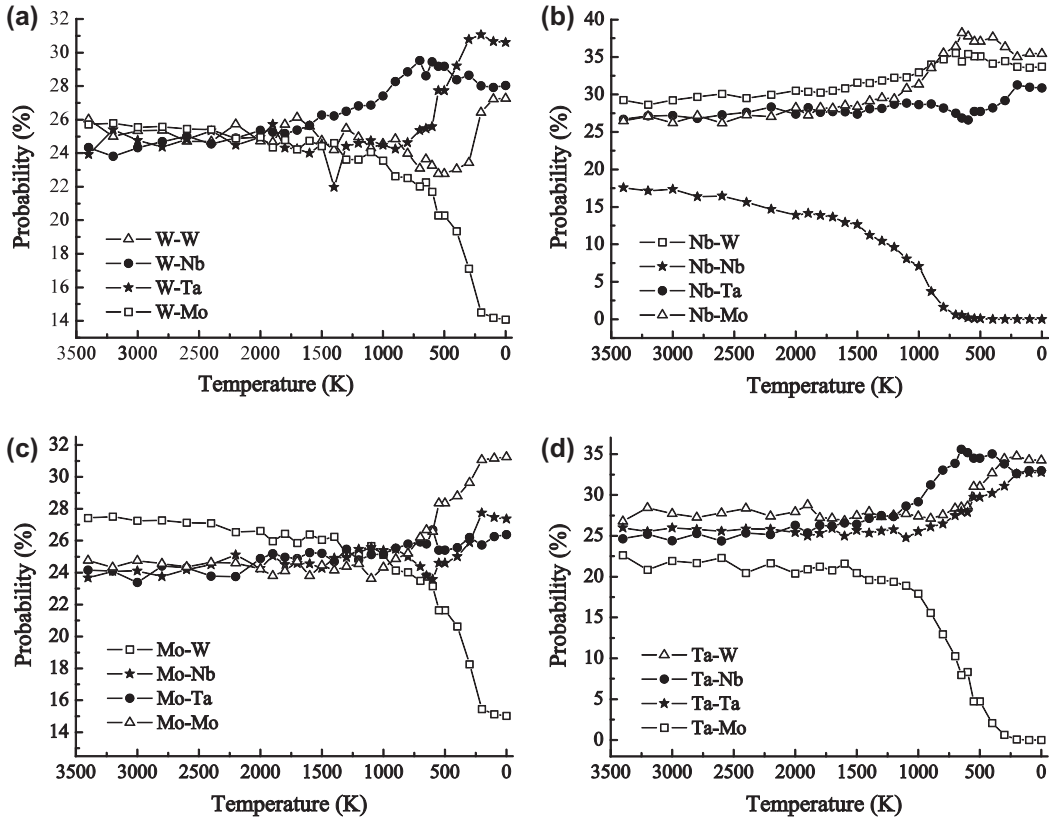

Fig. 2. Short-range matrix elements ρ (see text) between nearest-neighbors for (a) W, (b) Nb, (c) Mo, and (d) Ta as function of temperature for the $W_{27.3}Nb_{22.7}Mo_{25.6}Ta_{24.4}$ alloy.

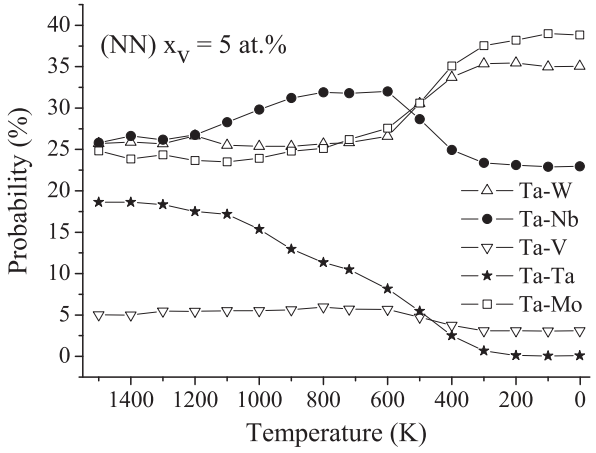

Fig. 3. Short-range order matrix elements ρ for the $W_{21.1}Nb_{20.6}Mo_{21.7}Ta_{15.6}V_{21.0}$ alloy.

For lower temperatures there is one single feature, common to all cases, which can be understood as partitioning of the different elements to each sublattice in the bcc structure: V and Nb in one, W and Mo in the other. The only low temperature feature is the behavior of Ta, the only element present in both sublattices, underscoring the particular strength of V–Ta bonds, as wherever Ta is, there will be V in a nearest-neighbor site. While it is not correct to say that this system is featureless, it can be certainly be said to be so in comparison to the 4-element case, which can be taken as an indication that with 5 elements in nearly equal amounts the high entropy of mixing effect dominates, leading to a disordered solid solution.

4.2. Transitional chains: addition of a fifth element to quaternary alloys

The experimental work of Senkov et al. [40] focuses on the addition of a specific amount of V to W–Nb–Mo–Ta alloys, raising the question of whether other transitional chains exhibit similar behavior. It is useful to examine all the possible transitions by any quaternary alloy with those elements to the corresponding five-element alloy (this being the one studied experimentally [40]). In this section, results of simulated annealing of the transitional alloys WNbMoTa + V are discussed, in addition to the other transitional chains: NbMoTaV + W, MoTaVW + Nb, TaVWNb + Mo, and VWNbMo + Ta. The ideal cases would refer to X additions to equiatomic quaternary alloys. However, slight departures from this case will be studied, in order to examine the specific role that each element has in fine changes, if any, in the phase structure of the transitional 5-element alloys. Table 2 summarizes the intermediate compositions in each transitional set, while Fig. 4 shows some details of the phase structure as seen in the simulation results for the different alloys in each chain (i.e., varying the concentration of the fifth element). All simulations show that each system transitions from a quaternary to a 5-element solid solution but, depending on the individual departures from the equiatomic case and the majority element, slight changes can be seen in terms of short range order or hints of precipitate formation in the path towards achieving the final composition. The most relevant information that can be extracted from these simulations is the particular role that the relative proportion of V and Ta play in each case. When abundant, there is a strong tendency towards Ta–V alloying, whereas when they are not, several domains can be identified in the computational cell with different compositions. As described in Section 3, it should be remembered that the calculations were made in cells

Table 2
Composition (in at.%) of each one of the alloys considered in the WNbMoTa + V transitional chain. In the other transitional chains, V takes the role of each of the other elements, while the substituted element takes the role of V.

W–Nb–Mo–Ta + V				
V	W	Nb	Mo	Ta
0	27.30	22.70	25.60	24.40
2.5	26.56	22.45	25.14	23.35
5.0	25.81	22.21	24.67	22.31
7.5	25.09	21.95	24.20	21.26
10.0	24.35	21.69	23.74	20.21
12.5	23.60	21.45	23.29	19.16
15.0	22.87	21.20	22.82	18.12
17.5	22.13	20.94	22.36	17.07
20.0	21.39	20.70	21.89	16.02
22.5	20.66	20.45	21.52	14.96
25.0	19.92	20.19	20.96	13.93

with uniform temperature-dependent lattice parameter, and that the phases described correspond to specific domains within the computational cell with their own atomic distribution, which may or may not be a faithful representation of the actual phase structure derived from experiment. However, lacking experimental evidence to confirm these results, the only purpose in discussing these modeling results is to show how the atomic distributions change with concentration until they reach the high entropy regime where the solid solution dominates. Together with eventual experimental evidence to confirm or not these results, initial guesses of the phase field of the solid solution could be made, but as it will be seen later, this information could more effectively be used as input for a modeling tool for achieving this goal.

The simulations, which are supposed to provide a reasonable representation of experimental results [4], yield a solid solution with slight changes in concentration in different regions of the alloy for all concentrations of V. These results are a manifestation of a trend (inhibited by limited diffusion) towards the formation of specific second phases. In what follows, the notation $(A,B)_C$ denotes a sublattice of the bcc structure populated primarily by A and, to a lesser extent, B. The subindex C denotes that C atoms are in solution, randomly scattered among A- or B-rich regions of the sublattice. Fig. 4 shows a succinct summary of the main results. All five transitional chains (from either quaternary to the final WNbMoTaV alloy) are shown in terms of the concentration x of the fifth element. The first row (for $x = 0$) indicates the phase structure of the different quaternary alloys. The 5-element system transitions through different atomic distributions as the concentration of the fifth element increases (solid arrow in Fig. 4), until a final structure is reached. At that point (11 at.% V for the first chain, 9 at.% Nb for the second, etc.), each system transitions (dashed arrow) to the solid solution (Mo,W,Ta)(V,Nb,Ta) that describes the high entropy 5-element alloy, without any further changes in its phase structure. The intermediate results (before the transition) display quite

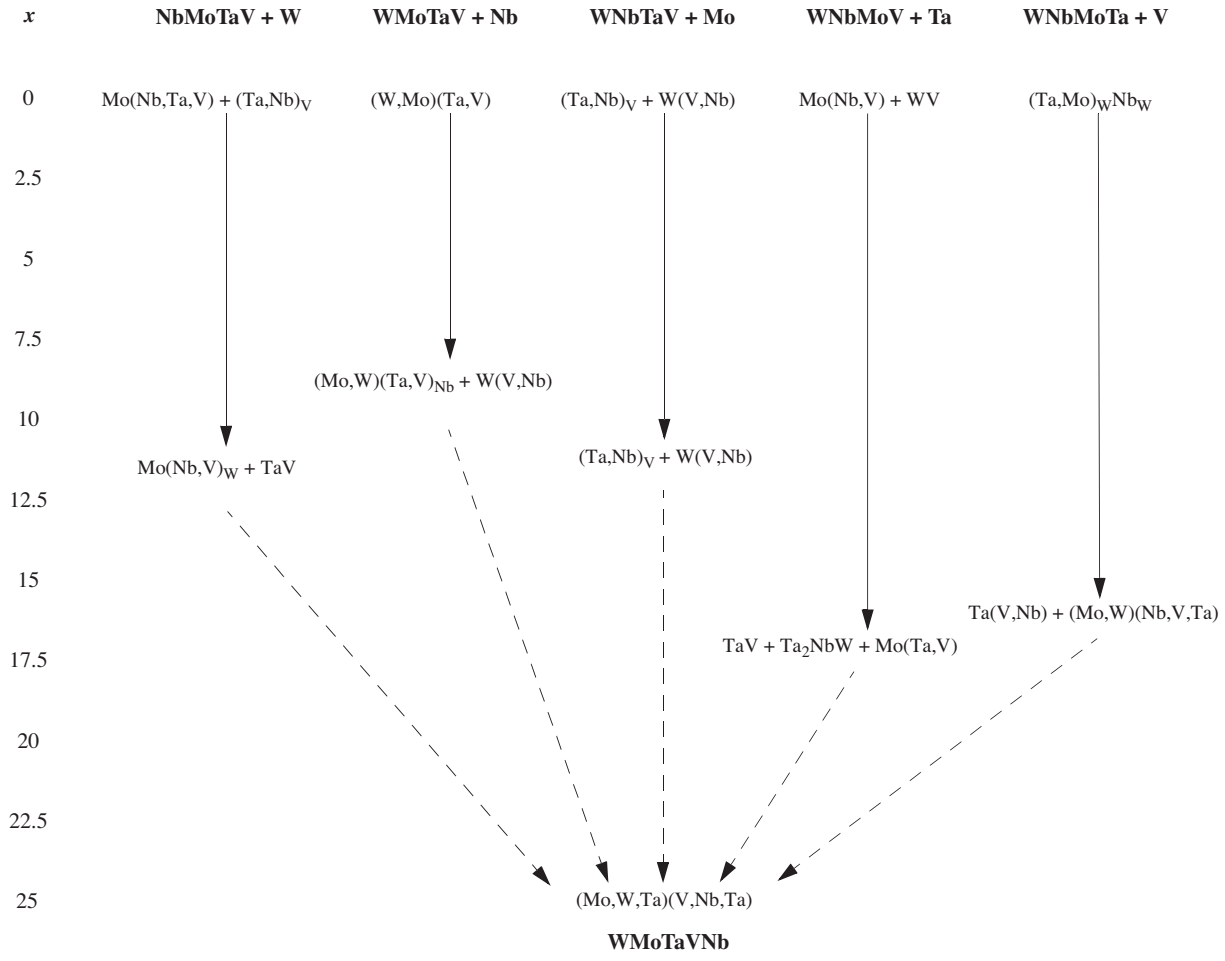

Fig. 4. Evolution of the different quaternary alloys to the W–Nb–Mo–Ta–V HEA. Each column describes the phase structure as a function of the concentration of the fifth element (x, in at.%). The arrows indicate a range of x for which no major changes in structure are seen. Each initial quaternary alloy and the five element alloy are noted at the top and bottom, respectively (see Table 1 for details). Solid arrows indicate transitions through different phase structures (detail not shown) and the entries at the lower end indicate the essential features before the transition to a solid solution (denoted by broken arrows).

different phase structures for each alloy. For example, in the NbMoTaV + W case, the system separates into a clear TaV domain and a $Mo(Nb,V)_W$ (where one plane is Mo-rich and the other has mostly Nb and V, with W partitioning to that sublattice). Other chains show other phase structures before the high entropy transition, in all cases displaying the superposition of two or three phases. All, however, transition to a solid solution at the indicated concentrations of the fifth element, where the two bcc sublattices are populated in the order indicated.

The most significant feature in all these cases is the interaction between Ta and V, and the way it affects the structure of the alloyas the proportion between them changes. A detailed description of the energetics, on an atom-by-atom basis, could be helpful in understanding the transition to the high entropy regime, but as it will be seen in the following section, an algorithm for determining the lower bounds for the concentration of each element can be determined based solely on bulk properties of each transitional chain.

5. Determining the transition to the high entropy regime

Based on the behavior described in Section 4, and focusing again on the alloy studied experimentally, it is then expected that Ta will play a significant role in the evolution of these alloys, and that its role will be enhanced (in the 5-element case) by the presence of V. Significant ordering trends, characteristic of the low temperature regime, compete with the underlying principle of HEA, where equal amounts of each element favor the formation of a continuous solid solution. This suggests that the transition to a high entropy regime could be better illustrated by focusing first on alloys with varying V concentration (keeping the remaining four elements in nearly equimolar amounts). To this effect, simulations of WNbMoTa + V alloys, with V contents ranging from 0 to 25 at.% (in steps of 2.5 at.%) were performed (see Table 2), and quantities such as the equilibrium lattice parameter (a_e), cohesive energy (E_c), and bulk modulus (B_0) as a function of temperature were determined in each case. As shown in Ref. [45], all curves $a_n(T)$, describing the evolution of the lattice parameter a_e for the different alloys with varying V concentration can be easily fitted to an analytical function with four independent parameters (A_1, A_2, T_0, p) which depend on the concentration of V:

$$a_n(T) = A_2 + \frac{A_1 - A_2}{1 + \left(\frac{T}{T_0}\right)^p}. \quad (2)$$

Two of these parameters (T_0 and p) can be used to determine the location of the inflexion point in these curves. This point can be then said to define the aforementioned 'critical temperature' (see Section 3.1), T_c, given by:

$$T_c = T_0 \left(\frac{p-1}{p+1}\right)^{\frac{1}{p}} \quad (3)$$

The numerical values of A_1, A_2, T_0, p and the resulting values of T_c for W–Nb–Mo–Ta–V alloys with varying V concentration are listed in Table 3. Similar functions can be used to fit the results for the cohesive energy and bulk modulus as a function of temperature for different concentrations of V.

It is important to note that as a function of V concentration (x_V), T_c exhibits a clear maximum value separating two distinct regimes. For this particular alloy, such value is $x_V^c = 9.38$ at.%. For smaller values of x_V^c, there is a steady linear increase in T_c with increasing V concentration, but this is reversed beyond this critical value, suggesting that this is a critical concentration for which the system transitions to a regime where the concentration of V is sufficiently high to let the high entropy behavior dictate the structure of the alloy. A detailed analysis of the temperature-dependent coordination matrix elements (shown in Figs. 2 and 3) indicates that, not surprisingly, the values of T_c are highly dependent on the onset of Ta–V interactions leading to the elimination of the solid solution regime with descending temperature. The presence of this critical point is not only perceived in the behavior of the lattice parameter, but also arises from the analysis of the behavior of E_c and B_0, making any of these quantities equally useful to describe the behavior of the system.

Table 3
Values of the fitting parameters A_1 (in Å), A_2 (in Å), T_0 (in K), p and the resulting values of T_c (in K) (see Eqs. (2) and (3))) for W–Nb–Mo–Ta–V alloys with varying V concentration (x_V, in at.%).

x_V	A_1	A_2	T_0	p	T_c
0	3.227	3.233	834.130	2.689	623.864
2.5	3.224	3.230	871.240	2.971	688.258
5	3.221	3.228	903.608	3.248	742.789
7.5	3.218	3.225	899.867	3.718	775.848
10	3.215	3.222	883.209	3.935	773.951
12.5	3.212	3.219	855.497	4.176	761.092
15	3.209	3.216	825.968	4.514	747.512
17.5	3.205	3.212	799.065	4.475	721.868
20	3.202	3.209	745.000	4.601	676.804
21	3.200	3.207	740.230	4.788	677.498
22.5	3.198	3.205	730.586	5.065	675.096
25	3.194	3.201	701.862	5.277	652.648

A similar analysis for the other transitional chains from a quaternary to a 5-element alloy, as discussed in Section 4.2, shows that regardless of the composition of the initial quaternary case, the addition of a fifth element results in behavior similar to that described above for the WNbMoTa + V case, in the sense that, for any concentration of the fifth element, the evolution of the lattice parameter, cohesive energy, or bulk modulus have the same functional form as that indicated in Eq. (2). However, there are differences in the resulting values for T_c as a function of concentration of the fifth element, and therefore resulting on a different critical concentration for the fifth element. For the chains corresponding to W, Nb, and Mo additions, the rather inert nature of these elements translates into a different shape for T_c, as shown in Fig. 5. As opposed to the V chain, where T_c had a clear maximum at the critical concentration (x_V = 9.38 at.%), the corresponding curves for W, Nb and Mo additions show a steady decrease in T_c with increasing temperature, which can be taken as an indication that neither one of these elements plays an important role in the final phase structure of the alloy. In other words, were it not for the interactions between Ta and V, additions of W, Nb or Mo would not alter the fundamental behavior that is already present in the corresponding quaternary cases (Nb–Mo–Ta–V for W additions, W–Mo–Ta–V for Nb additions, and W–Nb–Ta–V for Mo additions). This is equivalent to stating that these additions would not favor the formation of second phases as the temperature decreases, staying mostly in solution, and thus conserving the high entropy characteristics of the equimolar quaternary HEA. For W and Mo additions, the minimum in T_c occurs for $x_{W(or\ Mo)} \sim 20$ at.%, which corresponds to the equiatomic 5-element alloy. This is not so for Nb, which exhibits a minimum at approximately $x_{Nb} \sim 11.5$ at.%, probably due to the fact that in this chain the abundance of Nb facilitates the formation of a WV precipitate. Large additions of W, Nb or Mo to the corresponding quaternary alloys do not introduce any further changes in the phase structure or the high entropy behavior already present.

The case WNbMoV + Ta is somewhat different, highlighting the important role that Ta plays in the phase structure of the alloy for different concentrations. A critical concentration can be defined for this case, at about $x_{Ta} \sim 5$ at.% (see Fig. 5), but it is worth noting that, in contrast to the WNbMoTa + V case, additions of Ta to W–Nb–Mo–V have a more interesting role. First, for very low Ta concen-

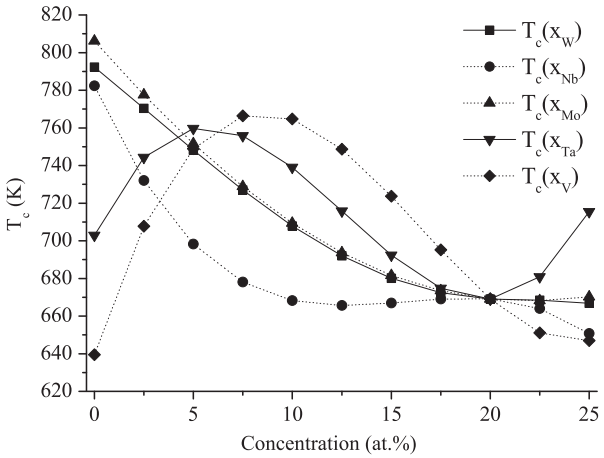

Fig. 5. Critical temperature T_c (in K) as a function of concentration of the fifth element (E) in the chain ABCD + E. Squares, circles, upward and downward triangles and diamonds correspond to the NbMoTaV + W, WMoTaV + Nb, WNbTaV + Mo, WNbMoV + Ta, and WNbMoTa + V, respectively.

tration, the system evolves as in the cases with Nb, Mo, and W additions, decreasing the critical temperature. This is a consequence of the partitioning of Ta to both sublattices. While this is hardly a high entropy situation (x_{Ta} < 5 at.%), it is apparent that this role of Ta (at low concentration) has an important effect on the evolution of the phase structure. Beyond this point, T_c decreases, until it reaches a minimum for the equiatomic case (x_{Ta}∼20 at.%). Up to this point, the behavior of Ta in W–Nb–Mo–V is not too different from that of V in W–Nb–Mo–Ta, which is to be expected due to the relevance of Ta–V interactions. It is for higher Ta concentration that differences exist: in the case of V additions to W–Nb–Mo–Ta, the critical temperature continues its descent, but in the case of Ta additions to W–Nb–Mo–V, it rises rapidly, indicating that excess Ta (above 20 at.%) is the driving force for further changes in the phase structure, departing from the solid solution characteristic of the equiatomic case.

Summarizing, the critical concentrations of the fifth element for each transitional chain, (understanding that this is the minimum amount of this element needed to ensure high entropy behavior for the 5-element alloy with the balance equally distributed amongst the other four elements) are x_V = 9.38 at.% for WNbMoTa + V, x_{Ta} = 5 at.% for WNbMoV + Ta, and zero for the remaining three chains, meaning that the additions of W to NbMoTaV, Nb to WMoTaV or Mo to WNbTaV will not alter the phase structure already present in the corresponding quaternary cases.

6. Conclusions

Atomistic modeling of 4- and 5-elements alloys suggests that it is possible to quantify the transition to the high entropy regime characterized by the formation of a continuous solid solution. The example presented indicates that it is possible to extract information regarding this transition from a detailed analysis of the evolution of the phase structure and individual atomic interactions, in spite of the limitation introduced by using a rigid computational cell. However, the introduction of the concept of a critical concentration suggests that it is also possible to understand the transition based mostly on the evolution of bulk physical properties, regardless of the individual interactions. There is, at this point, no experimental confirmation of the existence of the critical concentration, other than the fact that the modeling results are consistent with experimental results for those cases where experimental evidence exists. Its definition, however, suggests that it might be a useful design tool when considering alloys with a large number of elements, as it is the case with most HEA.

In the particular case of the 5-element W–Nb–Mo–Ta–V alloy, this concept identified the critical amount of the fifth element (x_V^c) needed to be added to the quaternary alloy in order to transition to a bcc solid solution, which is not immediately apparent from the analysis based only on atomic interactions. Due to the simplicity of the approach, it would then have the potential to be a practical tool for determining, given a certain mix of arbitrary number of elements, the necessary minimum concentration of each element needed to achieve typical high entropy behavior.

Acknowledgment

Fruitful discussions with N. Bozzolo are gratefully acknowledged.

References

[1] G. Bozzolo, J. Ferrante, J.R. Smith, Phys. Rev. B 45 (1992) 493.
[2] G. Bozzolo, J. E. Garcés, in: D.P. Woodruff (Ed.), The Chemical Physics of Solid Surfaces, Elsevier, 2002, pp. 30.
[3] G. Bozzolo, J. Khalil, R.D. Noebe, Comp. Mater. Sci. 24 (2002) 457.
[4] A. Wilson, G. Bozzolo, R.D. Noebe, J. Howe, Acta Mater. 50 (2002) 2787.
[5] H.O. Mosca, G. Bozzolo, M.F. del Grosso, Mat. Sci. Eng. B 162 (2009) 99.
[6] M.F. del Grosso, H.O. Mosca, G. Bozzolo, Intermetallics 18 (2010) 945.
[7] G. Bozzolo, H.O. Mosca, A.M. Yacout, G. Hofman, J. Nucl. Mater. 407 (2010) 228.
[8] A. Peker, W.L. Johnson, Appl. Phys. Lett. 63 (1993) 2342.
[9] J.W. Yeh, S.K. Chen, S.J. Lin, J.Y. Gan, T.S. Chin, T.T. Shun, C.H. Tsau, S.Y. Chang, Adv. Eng. Mater. 6 (2004) 299.
[10] J.W. Yeh, Annales de Chimie Science des Materiaux 31 (2006) 633.
[11] B. Cantor, I.T.H. Chang, P. Knight, A.J.B. Vincent, Mat. Sci. Eng. 375–377 (2004) 213.
[12] X.F. Wang, Y. Zhang, Y. Qiao, G.L. Chen, Intermetallics 15 (2007) 357.
[13] Y.J. Zhou, Y. Zhang, Y.L. Wang, G.L. Chen, Appl. Phys. Lett. 90 (2007) 181904.
[14] Y.J. Zhou, Y. Zhang, Y.L. Wang, G.L. Chen, Mat. Sci. Eng. A 454–455 (2007) 260.
[15] C.C. Tung, J.W. Yeh, T.T. Shun, S.K. Chen, Y.S. Huang, H.C. Chen, Mater. Lett. 61 (2007) 1.
[16] C. Li, M. Zhao, J.C. Li, Q. Jiang, J. Appl. Phys. 104 (2008) 113504.
[17] B.S. Li, Y.P. Wang, M.X. Ren, C. Yang, H.Z. Fu, Mat. Sci. Eng. A 498 (2008) 482.
[18] S. Varalakshmi, M. Kamaraj, B.S. Murty, J. All. Compd. 460 (2008) 253.
[19] J.H. Pi, Y. Pan, L. Zhang, H. Zhang, J. All. Compd. 509 (2011) 5641.
[20] C. Li, J.C. Li, M. Zhao, Q. Jiang, J. All. Compd. 475 (2009) 752.
[21] T.T. Shun, C.H. Hung, C.F. Lee, J. All. Compd. 493 (2010) 105.
[22] L.H. Wen, H.C. Kou, H. Chang, X.Y. Xue, L. Zhou, Intermetallics 17 (2009) 266.
[23] K.C. Hsieh, C.F. Yu, W.T. Hsieh, W.R. Chiang, S.S. Ku, J.H. Lai, C.P. Tu, C.C. Yang, J. All. Compd. 483 (2009) 209.
[24] H.P. Chou, Y.S. Chang, S.K. Chen, J.W. Yeh, Mat. Sci. Eng. B 163 (2009) 184.
[25] Z. Hu, Y. Zhan, G. Zhang, J. She, C. Li, Mater. Design 31 (2010) 1599.
[26] C.M. Lin, H.L. Tsai, J. All. Compd. 489 (2010) 30.
[27] S. Varalakshmi, M. Kamaraj, B.S. Murty, Mat. Sci. Eng. A 527 (2010) 1027.
[28] S. Varalakshmi, M. Kamaraj, B.S. Murty, Met. Mat. Trans. A 41 (2010) 2703.
[29] C.Y. Hsu, T.S. Sheu, J.W. Yeh, S.K. Chen, Wear 268 (2010) 653.
[30] C.Y. Hsu, C.C. Juan, W.R. Wang, T.S. Sheu, J.W. Yeh, S.K. Chen, Mat. Sci. Eng. A 528 (2011) 3581.
[31] Y.F. Kao, S.K. Chen, T.J. Chen, P.C. Chu, J.W. Yeh, S.J. Lin, J. All. Compd. 509 (2011) 1607.
[32] S. Singh, N. Wanderka, B.S. Murty, U. Glatzel, J. Banhart, Acta Mater. 59 (2011) 182.
[33] H. Zhang, Y. Pan, Y. He, H. Jiao, Appl. Surf. Sci. 257 (2011) 2259.
[34] C.D. Gómez-Esparza, R.A. Ochoa-Gamboa, I. Estrada-Guel, J.G. Cabañas-Moreno, J.I. Barajas-Villarruel, A. Arizmendi-Morquecho, J.M. Herrera-Ramírez, R. Martínez-Sánchez, J. All. Compd. 509 (Supplement 1) (2011) S279.
[35] L.M. Wang, C.C. Chen, J.W. Yeh, S.T. Ke, Mater. Chem. Phys. 126 (2011) 880.
[36] J.W. Yeh, Y.L. Chen, S.J. Lin, S.K. Chen, Mater. Sci. Forum 560 (2007) 1.
[37] Y. Zhang, Y. Zhou, Mater. Sci. Forum 561–565 (2007) 1337.
[38] F.J. Wang, Y. Zhang, G.L. Chen, J. All. Compd. 478 (2009) 321.
[39] C.H. Zhang, M.H. Lin, B. Wu, G.X. Ye, L.K. Zhang, T. Chen, W.J. Zhang, Z.H. Zheng, Y.Q. Shao, B.Y. Zhou, C. Wang, J. Shangai Jiaotong Univ. (Sci.) 16 (2011) 173.
[40] O.N. Senkov, G.B. Wilks, D.B. Miracle, C.P. Chuang, P.K. Liaw, Intermetallics 18 (2010) 1758.
[41] O.N. Senkov, G.B. Wilks, J.M. Scott, D.B. Miracle, Intermetallics 19 (2011) 698.
[42] O.N. Senkov, J.M. Scott, S.V. Senkova, D.B. Miracle, C.F. Woodward, J. All. Compd. 509 (2011) 6043.
[43] J. Smith, T. Perry, A. Banerjea, J. Ferrante, G. Bozzolo, Phys. Rev. B 44 (1991) 6444.
[44] P. Blaha, K. Schwarz, G.K.H. Madsen, D. Kvasnicka, J. Luitz, WIEN2K, an Augmented Plane Wave + Local Orbitals Program for Calculating Crystal Properties, Karlheinz Schwarz, Techn. Universität Wien, Austria, 2001, ISBN 3-9501031-1-2.
[45] M.F. del Grosso, G. Bozzolo, H.O. Mosca, Physica B (2012), http://dx.doi.org/10.1016/j.physb.2011.12.088.